SUPPORTING INFORMATION FOR:

Cooper, D. and T. Gutowski. 2018. Prospective environmental analyses of emerging technology: A critique, a proposed methodology, and a case study on incremental sheet forming. *Journal of Industrial Ecology.*

Summary

This supporting information provides information useful to understanding the themes and numbers introduced in the main manuscript. This document is 21 pages long and contains 6 tables and 12 figures.

1: Recent publications on prospective environmental analyses of emerging technology

Table S1 presents a representative sample of recent publications on the anticipated environmental impacts of an emerging technology, including the technology studied and the boundaries of the analysis.

Authors	Technology studied	Boundaries of analysis
Brodrick (2010)	U.S. energy savings from the use of energy-efficient solid state lighting (SSL)	The analysis attempts to incorporate realistic adoption scenarios: the analysis considers the costs and efficiencies of conventional and SSL technologies and how they are likely to develop over time. The analysis examines potential energy savings in the use phase only and does not examine potential rebound effects.
Levy et al. (2016)	U.S. energy savings and emissions reductions from the use of increased insulation in new homes	The analysis looks at the energy savings in the use phase only and does not attempt to look at potential rebound effects. The paper does examine costs considerations. For example, it is stated that increasing residential insulation from current code levels for all new homes would cost approximately $380 million. However, adoption scenarios and cost models are not studied in detail.
DeForest et al. (2015)	U.S. energy savings and carbon emissions reductions from the use of a transparent,	This analysis considers potential energy savings in the use phase only (within buildings) and does not consider manufacturing energy requirements. Cost

	near-infrared switching electrochromic window glazing for building applications. These glazings can modulate the transmission of heat without affecting transmission of visible light	considerations are mentioned but not modeled. Rebound effects are not considered, nor are a range of realistic adoption scenarios.
Shehabi et al. (2013)	U.S. energy savings potential from dynamic daylighting control glazings; using dynamic prismatic optical element window coatings to continuously readjust incoming light to maximize the performance and energy savings available from daylighting controls	This analysis considers potential energy savings in the use phase; for example, by allowing light to penetrate more deeply into the building interior (potentially saving on electricity used for artificial light). The analysis does not consider manufacturing energy requirements. Cost considerations are mentioned but not modeled. Rebound effects are not considered, nor are a range of realistic adoption scenarios.
Huang et al. (2015)	U.S. energy reductions and GHG emissions avoided by 2050 from the use of additive manufacturing to make components for aircraft	In this analysis both embodied (manufacturing) and use phase energy requirements are considered. Adoption scenarios are modeled using the Bass model. Cost considerations are also mentioned but not modeled. Rebound effects are not considered.
Das et al. (2016)	U.S. energy reductions from using lightweight materials in light-duty vehicles	In this analysis both embodied (manufacturing) and use phase energy requirements are considered. Adoption scenarios are modeled using the Bass model. Cost considerations are also mentioned but not modeled. Rebound effects are not considered.
Greenblatt and Saxena (2015)	U.S. greenhouse-gas (GHG) emission reductions from the use of autonomous taxis	GHG emission reductions are calculated in this paper using 3 key assumptions: (1) de-carbonization of the future electricity grid; (2) smaller vehicle sizes resulting from trip-specific autonomous vehicle deployment; (3) increased vehicle-miles traveled, combined with lack of labor costs, making energy efficiency (especially battery-electric vehicles) commercially attractive. This paper does not discuss the environmental impacts of manufacturing autonomous or conventional vehicles, nor

	does it consider the potential for rebound effects.

Table S1: Recent publications on prospective environmental benefits (typically in the United States) of an emerging technology

2: Lead-time for different sheet metal forming processes

Figures S1-S3 show contours representing the total time needed to deliver 20, 250, and 2000 identical parts respectively. The varying production rate and tool lead times of each process have been examined by undertaking extensive literature reviews combined with semi-structured interviews with industry experts. Full details with references are presented in Rossie's (2015) thesis. The ISF tooling lead time is shown to be very low and often only determined by the time needed to generate a tool path. Although this is typically the case it should be noted that the lead time can be longer when a new ISF forming tool geometry is required in order to form different depths of parts or in order to form different materials. It can be seen in Figure S1 that for very small batches of parts (20 units or less) RAFFT can produce the full batch in around 2 weeks or less. This represents a significant lead-time saving compared to drawing, which requires over 6 weeks.

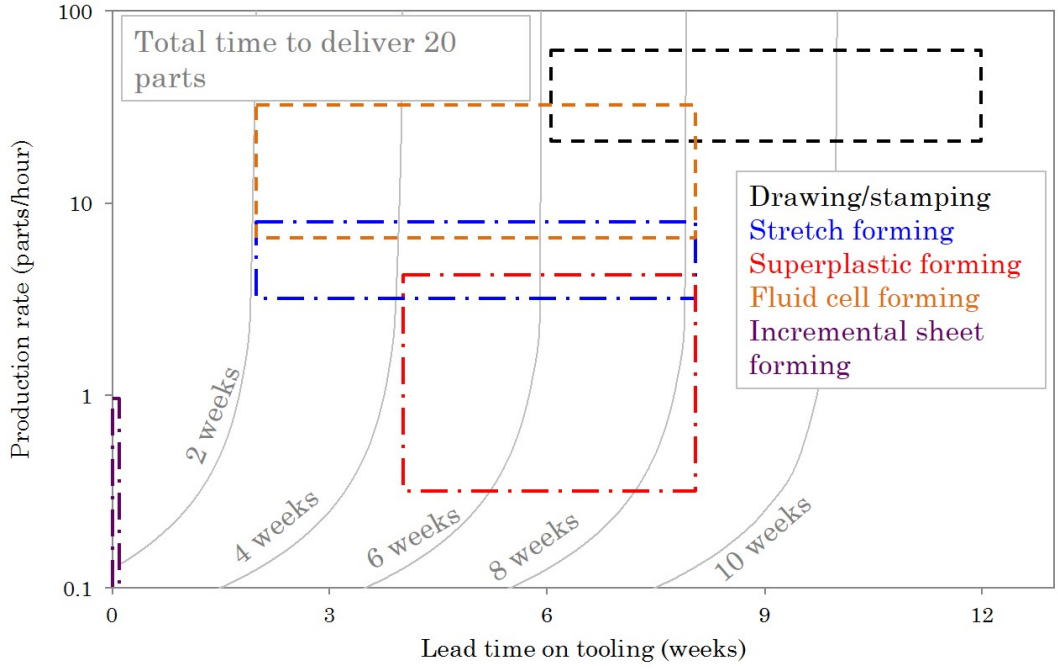

Figure S1: The total time needed to deliver a batch of 20 identical parts using different SMF processes

Figure S2 shows that for batch sizes around 250 units the total time needed to produce the batch is comparable across the different SMF processes.

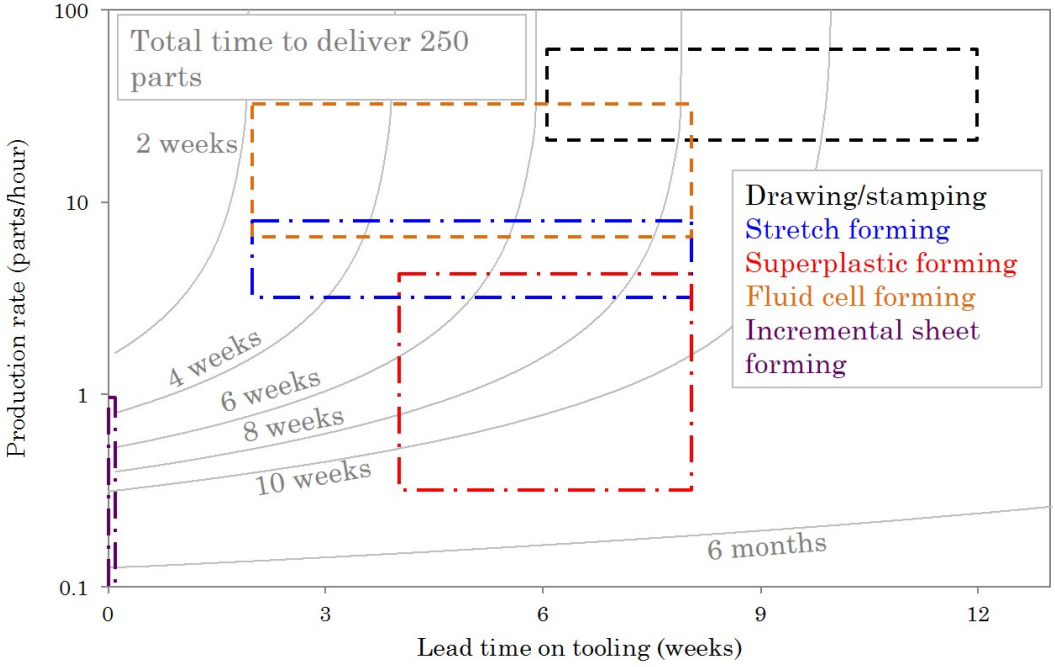

Figure S2: The total time needed to deliver a batch of 250 identical parts using different SMF processes

Figure S3 shows that for batch sizes around 2,000 units (and over) the total time needed to produce the batch using RAFFT is longer than it would take using conventional matched zinc die drawing.

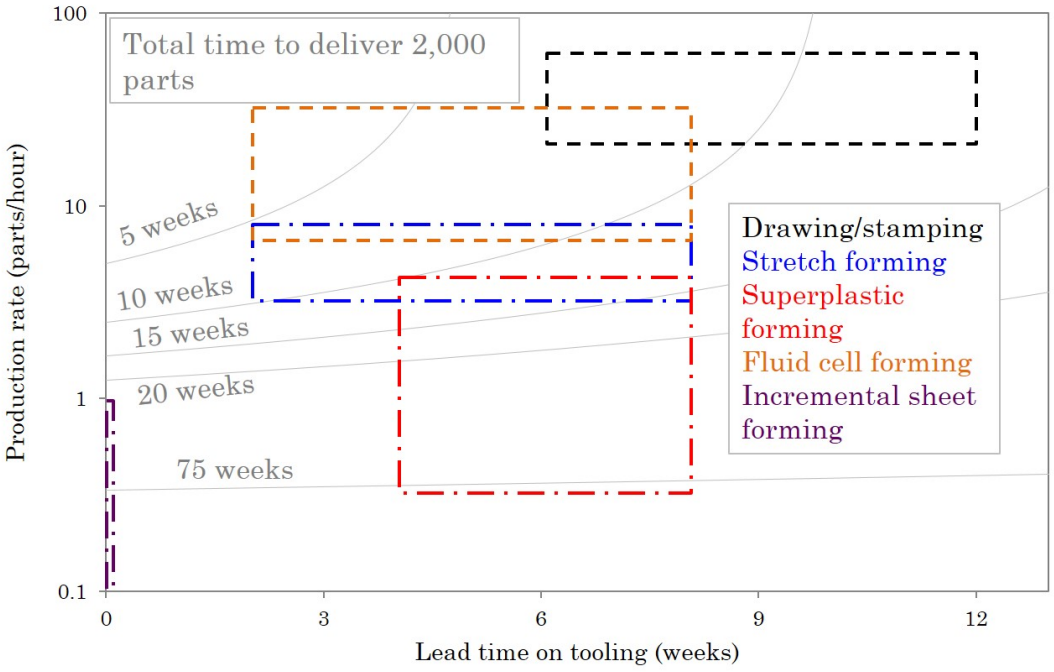

Figure S3: The total time needed to deliver a batch of 2,000 identical parts using different SMF processes

3: Technology level impacts—energy and cost models

This information is taken from Cooper et al. (2017) and Cooper and Gutowski (2016)

Environmental impacts (including energy requirements) are calculated from lifecycle inventories via the use of impact assessment methodologies, which use scientific knowledge to connect consumption and emissions with specific types of environmental and health degradation. The impacts considered here are cumulative energy demand (CED), also known as primary or embodied energy; cumulative carbon dioxide equivalents emitted, also known as embodied carbon dioxide, which is a measure of global warming potential (GWP) with a 100-year time horizon; and human health impacts in disability-adjusted life years (DALYs). The boundaries of the energy and cost analyses are shown in Figure S4. The impacts and costs are expressed "per part," with the impacts and costs of a die-set amortized (allocated equally) over the total number of parts produced using that die. The analyses are 'cradle-to-gate' life cycle assessments: each analysis starts from resource extraction (e.g., mining of ore, drilling for natural gas) and ends at the output of the forming process. In order to reduce confusion, in this report 'MJ' refers to the CED, and 'kWh' refers to metered electricity use.

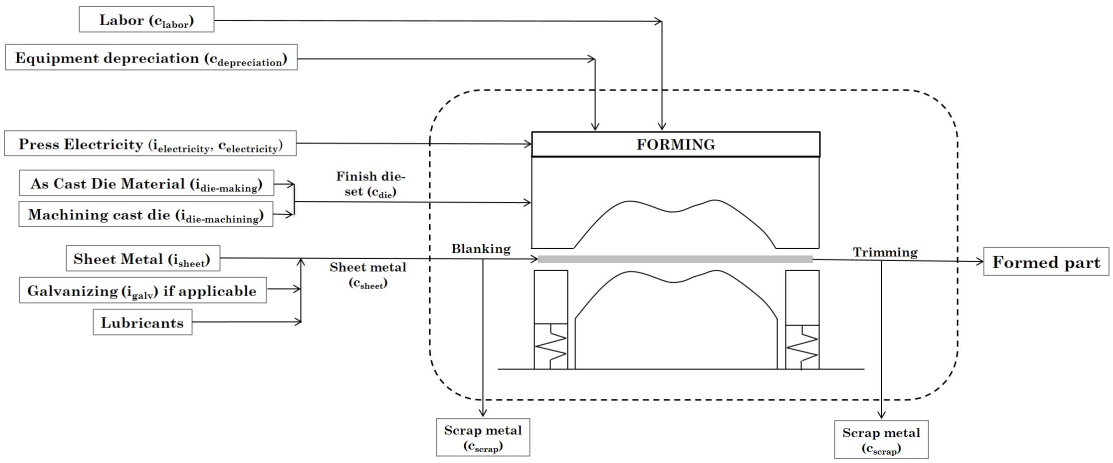

Figure S4: Boundaries of case study analyses: The ecological impacts (I_{xx}) and costs (C_{xx}) of forming sheet metal parts

The 'recycled content' method (also known as the 'cutoff' approach') is used for all analyses. With this approach, the fraction of recycled material in the material inputs, along with the impacts of primary and recycled (secondary) material production, is used to produce 'blended' impacts for each material input (see Table S2).

Inputs[1]	Density (ρ_{metal})	CED[2]	GWP	Human health	Costs	
Electricity	**N/A**	**MJ/kWh**	**kgCO_2e/kWh**	**DALY/kWh**	**USD/kWh**	
Medium voltage ($i_{electricity}$)	N/A	13	0.7	4.7E-07	0.07	
Sheet Metal (i_{sheet})	**kg/m³**	**MJ/kg**	**kgCO_2e/kg**	**DALY/kg**	**New – USD/kg**	**Scrap – USD/kg**
Low carbon steel sheet (r=0%)	7,850	31.3	2.5	3.2E-06	0.71	0.32
Generic alum. sheet (r=24.2%)	2,700	180.3	15.5	2.1E-05	2.55	1.54
Aluminum sheet (AA7075) r=24.2%	2,810	175.5	14.8	2.1E-05	2.55	1.54
Aluminum sheet (AA6014) r=24.2%	2,700	181.9	15.5	2.1E-05	2.55	1.54
Aluminum sheet (SP5083) r=24.2%	2,660	202.3	16.9	2.4E-05	7.65	4.63
Galvanization (for steel sheets)	**Thickness**	**MJ/m² sheet**	**kgCO_2e/m² sheet**	**DALY/m² sheet**	**USD/kg**	
Galvanizing (i_{galv})[3]	20-45 µm thick	82.1	5.3	1.8E-05	N/A[4]	
Lubricants	**kg/m³**	**MJ/kg**	**kgCO_2e/kg**	**DALY/kg**	**USD/kg**	
Lubricating oil	845	84.1	4.0	1.4E-06	5.5	
Graphite	959	59.1	4.7	6.7E-07		
As Cast Die Material ($i_{die\text{-}making}$)	**kg/m³**	**MJ/kg**	**kgCO_2e/kg**	**DALY/kg**	**USD/kg**	
Casting iron (r=65.7%)	7,150	30.9	2.0	3.1E-06	N/A[5]	
Casting zinc (r=97.5%)	6,920	16.4	1.0	9.7E-07		
Bulk Alum: AA7075 (r=24.2%)	2,700	164.9	14.2	2.0E-05		
RenShape 5166 (use and disposal) (r=0%)	1,700	78.4	3.1	2.5E-06		
Machining Listed Material ($i_{die\text{-}machining}$)	**kg/m³**	**MJ/kg$_{removed}$**	**kgCO_2e/ kg$_{removed}$**	**DALY/ kg$_{removed}$**	**USD/kg$_{removed}$**	
Cast iron	7,150	4.4	0.2	1.8E-07	N/A[5]	
Cast zinc	6,920	10.4	0.6	3.5E-07		
Bulk aluminum (AA7075)	2,700	6.9	0.4	3.3E-07		
RenShape[6] 5166	1,700	10.4	0.6	3.5E-07		

1. "r" refers to the recycled content of the material.
2. A CED value for electricity (13 MJ/kWh) corresponds to a conversion efficiency of 28%.
3. Impacts account for galvanizing on both sides of the sheet.
4. The prices for low carbon steel sheet include the cost of galvanization.
5. The cost of the making die-sets is addressed in Table S3.
6. In the absence of other data, it is conservatively assumed that the impacts for machining resin are equivalent to machining zinc.

Table S2: Intrinsic model input environmental and cost impacts (r: recycled content)

The global models constructed in this section allow environmental impacts to be estimated based on as little information as the process used, the number of parts produced over the die-set lifespan (N), final part material, surface area (X square meters, corresponding to one side), thickness (T meters), and depth (h meters).

Equation (S1) and equation (S2) present a simple representation of the impacts and costs per part. The impacts of the die are amortized over the total number of parts made using that tool (N).

$I_{per part} = I_{sheet} + I_{press\text{-}electricity} + \frac{I_{die}}{N}$	(S1)
$C_{per\ part} = (C_{sheet} - C_{scrap}) + C_{press\text{-}elec} + \frac{C_{die}}{N} + C_{dep} + C_{labor}$	(S2)

The die cost (C_{die}) is shown for each process in Table S3. The impacts of the sheet metal (I_{sheet}, C_{sheet}, C_{scrap}) and press electricity ($I_{press\text{-}electricity}$, $C_{press\text{-}elec}$), die (I_{die}), as well as the equipment depreciation costs (C_{dep}) and labor costs (C_{lab}), can be expressed as equations S3-S9, where α is the overall material yield from stock sheet to final part (ratio of mass of the part to mass of the stock sheet); ρ_{metal} is the density of the sheet metal (in kg/m^3); $W_{press\text{-}electricity}$ is the metered electrical energy needed to form a part (in kWh); M_{die} is the mass of the cast die (in kg); $M_{machined\text{-}away}$ is the mass of the cast die that is machined away to produce the final die shape (in kg); $Time_{attr.dep}$ is the amount of the cycle time that is attributable to equipment depreciation; and $Time_{attr.lab}$ is the amount of the cycle time that costs labor.

$I_{sheet} = \frac{X}{\alpha}\left[T\,\rho_{metal}\,i_{metal} + i_{galv}\right]$	(S3)
$C_{sheet} - C_{scrap} = \frac{XT\,\rho_{metal}}{\alpha}\left(c_{sheet} - c_{scrap}\,(1-\alpha)\right)$	(S4)
$I_{press\text{-}elec} = i_{elec} W_{press\text{-}elec}$	(S5)
$C_{press\text{-}elec} = i_{elec}\, c_{press\text{-}elec}$	(S6)
$I_{die} = i_{die-making} M_{die} + i_{die-machining} M_{machined-away}$	(S7)
$C_{dep} = c_{dep} \times Time_{attr.\,dep}$	(S8)
$C_{lab} = c_{lab} \times Time_{attr.\,lab}$	(S9)

Practitioners are free to fill in their own values where available. Otherwise, most of the intrinsic impacts and densities of the inputs (i_{metal}, i_{galv}, ρ_{metal}, $i_{electricity}$, $i_{die\text{-}making}$ and $i_{die\text{-}machining}$, c_{sheet}, c_{scrap}) are given in Table S2. Table S3 presents representative values for the other variables in equations S3-S9 (α, $W_{press\text{-}electricity}$, M_{die} and $M_{machined\text{-}away}$, C_{dep}, $Time_{attr.\,dep}$, $Time_{attr\,lab}$) as functions of the process and the final part shape. The precise values depend on many details of the part shape (e.g., whether the shape has holes or deep "features") and process machine architecture. Such details are neglected in favor of creating a simple model with uncertainty assigned to the variables (see Table S3).

	Drawing (hyd. press)	Stretch forming[1]	Fluid cell forming	Superplastic forming[1]	RAFFT[2]	Uncertainty[7,8]
Press electricity ($W_{press\text{-}electricity}$) [kWh/part]	1.2	$12.7+\left(\uparrow\frac{N}{B}\right)\times\left(\frac{27.5}{N}\right)$	$4.7\times\frac{X}{\alpha_{trim}}$	$(36300\,T)+\left(\uparrow\frac{N}{B}\right)\left(\frac{474\times X}{N\times\alpha_{trim}}\right)$	$0.7+10.3\frac{h\times\sqrt{X}}{v\times s}$	±50%
Cycle time (hours)	$\frac{2.8}{60}=0.05$	$\frac{9.8}{60}=0.16$	$\frac{6.5}{60}=0.11$	$\frac{15\times T}{60}=0.25T$	$\frac{25}{60}+3.03\frac{h\times\sqrt{X}}{v\times s}$	±25%
Attributable time to labor (hours/part)	$\left(\left(\uparrow\frac{N}{B}\right)\times\left(\frac{1}{N}\right)\right)+0.05$	$\left(\left(\uparrow\frac{N}{B}\right)\times\left(\frac{0.5}{N}\right)\right)+0.16$	$\left(\uparrow\frac{N}{B}\right)\left(\frac{2X}{3.01N\times\alpha_{trim}}\right)+\left(\frac{4.7X}{60\alpha_{trim}}\right)+\left(\frac{1.6X}{60\times3.01\alpha_{trim}}\right)$	228T	$\frac{25}{60}$	±50%
Attributable time to equipment depreciation (hours/part)	$\left(\left(\uparrow\frac{N}{B}\right)\times\left(\frac{1}{N}\right)\right)+0.05$	$\left(\left(\uparrow\frac{N}{B}\right)\times\left(\frac{0.5}{N}\right)\right)+0.16$	$\left(\uparrow\frac{N}{B}\right)\left(\frac{2X}{3.01N\times\alpha_{trim}}\right)+\left(\frac{4.7X}{60\alpha_{trim}}\right)+\left(\frac{1.6X}{60\times3.01\alpha_{trim}}\right)$	$\left(\uparrow\frac{N}{B}\right)\left(\frac{3\times X}{N\times\alpha_{trim}}\right)+228T$	$\frac{25}{60}+3.03\frac{h\times\sqrt{X}}{v\times s}$	±50%
Die material[3]	Zinc	Zinc	Zinc	Iron	N/A	N/A
Die mass (Md_{ie}) [kgs]	$4590\times\frac{X}{\alpha_{trim}}$	$1695\times\frac{X}{\alpha_{trim}}$	$2190\times\frac{X}{\alpha_{trim}}$	$1560\times\frac{X}{\alpha_{trim}}$	0	See Note 4
Die mass machined ($M_{machined\text{-}away}$) [kgs]	$0.15M_{die}$	$0.1M_{die}$	$0.1M_{die}$	$0.1M_{die}$	0	±25%
Overall material yield (α)	0.52	$\frac{0.9X}{X+0.86\sqrt{X}}$	0.64	0.36	$\frac{0.9X}{X\uparrow\text{frame area}}$	±35% to I_{sheet}
Blanking yield (α_{blank})	0.8	0.9	0.8	0.9	0.9	N/A
Trimming yield (α_{trim})	0.65	$\frac{X}{X+0.86\sqrt{X}}$	0.8	0.4	$\frac{X}{X\uparrow\text{frame area}}$	N/A
Die cost[5] (C_{die}) [USD]	$\left(4800\times\frac{X}{\alpha_{trim}}\right)+35000$	$\left(1740\times\frac{X}{\alpha_{trim}}\right)+12700$	$\left(2180\times\frac{X}{\alpha_{trim}}\right)+15900$	$\left(3048\times\frac{X}{\alpha_{trim}}\right)+22200$	0	See Note 6
Equipment depreciation (USD/hour)	42	120	370	25	20	±50%
Labor cost (USD/hour)	65	65	65	65	65	±50%

1. B is the number of parts produced during that batch. ↑ indicates rounding up the fraction, $\uparrow\left(\frac{N}{B}\right)$ up to the nearest integer. For SPF, B cannot be greater 100.
2. In the case of ISF, ↑ indicates rounding up to the nearest ISF square frame size area. h is part depth (meters), v is tool speed (meters per hour), s is tool vertical step size (meters, perpendicular to the plane of the blank). Nb: 10.3 factor in press electricity equals product of 3.4 kW aver. power draw & 3.03 constant of proportionality from cycle time calculation.
3. The labeled die materials assumes dies are cast & then machined. However, dies for small parts are often machined from stock metal blocks: steel for SPF, but likely aluminum or steel for the other processes.
4. Die mass- Drawing error: ±45%; Stretch forming error: ±90%; FCF error: ±90%; SPF error: ±90%; ISF error: 0%.
5. If a given die-set is made from resin, multiply final die cost by a factor of 0.6
6. Die cost- Drawing error: ±30%; Stretch forming error: ±90%; FCF error: ±50%; SPF error: ±90%; ISF error: 0%.
7. The uncertainty applied to both the sheet metal and electricity costs is ±55%. The relative increases in uncertainty reflect the relative variation in material and electricity costs.
8. The uncertainties are modeled as uniform distributions.

Table S3: Forming characteristics for different processes used in predictive global models

As a mature technology, drawing and FCF costs and impacts are stable and unlikely to substantially decline further. The premise of this article's case study analysis is the successful development of an ISF machine with the specifications described in Table 1 of the main paper, which would then represent a relatively mature technology. The cost of a successfully developed ISF process was evaluated using physical reasoning and knowledge of the sub-unit costs rather than by applying a learning curve. For example, the cost of equipment R&D was not included in ISF machine costs (which has exceeded 25% of total machine costs in the past), nor were the ISF costs and energy implications of try-out parts that in recent research have been formed and then scrapped. An alternative analysis could map these improvements onto a learning curve that would see incremental cost and impact reduction over the time period of interest.

4 Scale of technology deployment in 2030

As presented in equation 2 of the main manuscript, the distribution corresponding to the technical potential of ISF by 2030 (parts per year) is equivalent to the equation presented in equation S10.

$$X_{\text{Technical potential}}\ [parts/year] = 270 \times N(37,9) \times N(41,400) \quad \text{(S10)}$$

Both normal distributions in equation S10 are truncated below zero. $X_{\text{Technical potential}}$ was calculated by performing 10,000 simulations, each picking a number randomly from the distributions. The result is shown in Figure S5.

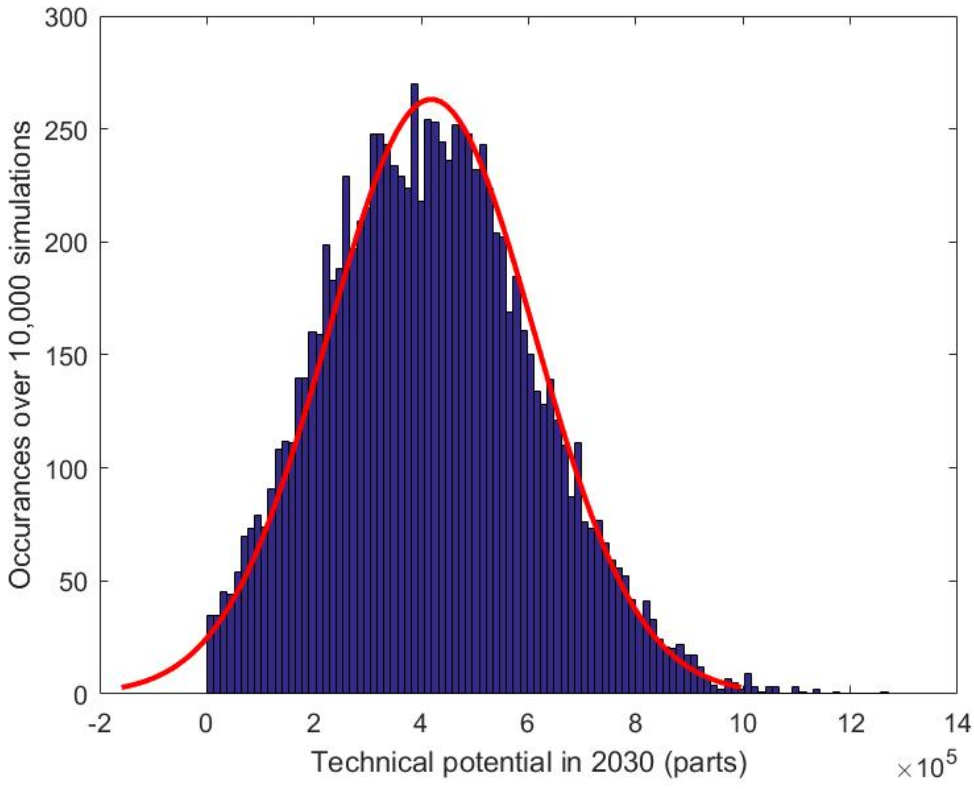

Figure S5: Technical potential (parts per year) of ISF by 2030. Distribution from 10,000 simulations

The distribution has a kurtosis of 2.9. The closest normal distribution (determined by Matlab) has a mean of 420,000 parts (consisting of 390,000 parts in 250-unit batches and 30,000 parts in 20-unit batches) and a standard deviation of 190,000 parts.

4.1 Energy and cost saving market size

20-unit batches of parts

As shown in Table 2 of the main manuscript, all parts made during part prototyping (20-unit batches) are cheaper and less energy intensive to form using ISF than zinc die drawing. Hence, the distribution for the number of parts (in 20-unit batches) for which ISF will save energy and money is given in equation S11.

$$X_{\text{20 unit batch energy \& cost saving potential}}\ [parts\ /\ year] \sim 20 \times N(37,9) \times N(41,400) \quad \text{(S11)}$$

The distribution was calculated by performing 10,000 simulations, each picking a number randomly from the distributions. The result is shown in Figure S6.

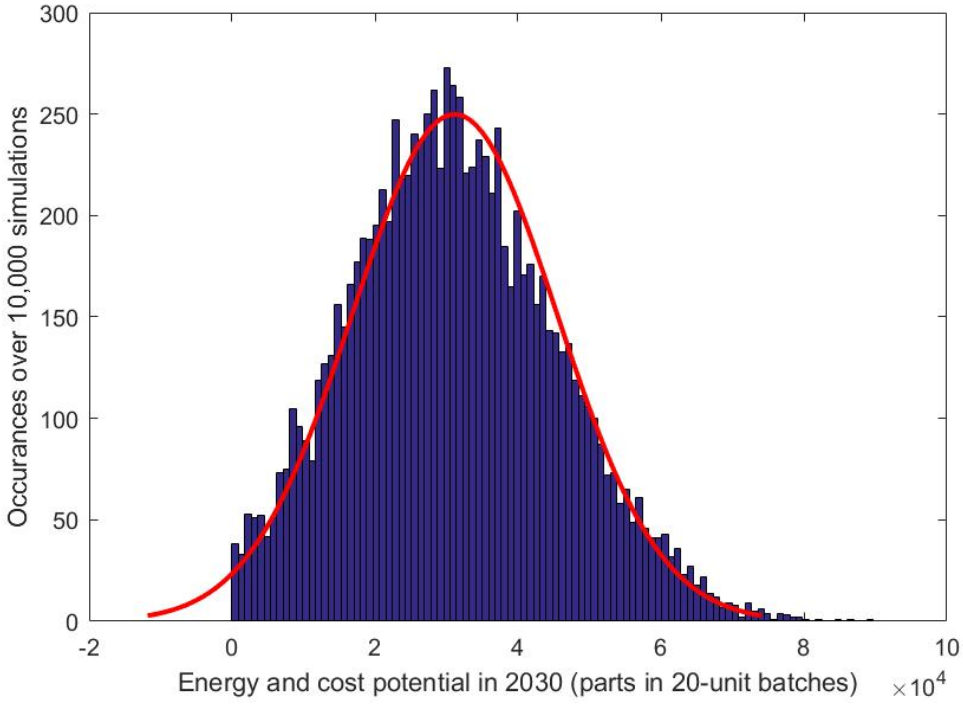

Figure S6: Energy and cost saving potential (parts per year) of ISF for 20-unit batches by 2030. Distribution from 10,000 simulations

The distribution has a kurtosis of 2.9. The closest normal distribution (determined by Matlab) has a mean of 30,000 parts and a standard deviation of 14,000 parts.

250-unit batches of parts

As shown in Table 2 of the main manuscript, 36 to 37 of the parts in a vehicle made during car development (250-unit batches) are less energy intensive to form using ISF than zinc die drawing. Hence, the distribution for the number of parts (in 250-unit batches) for which ISF will save energy is given in equation S12.

$$X_{Energysavingpotential\ \text{potential}\ 250-unitatches}\ [parts/year] = 250 \times N(36.5,0.25) \times N(41,400) \quad \text{(S12)}$$

The distribution was calculated by performing 10,000 simulations, each picking a number randomly from the distributions. The result is shown in Figure S7.

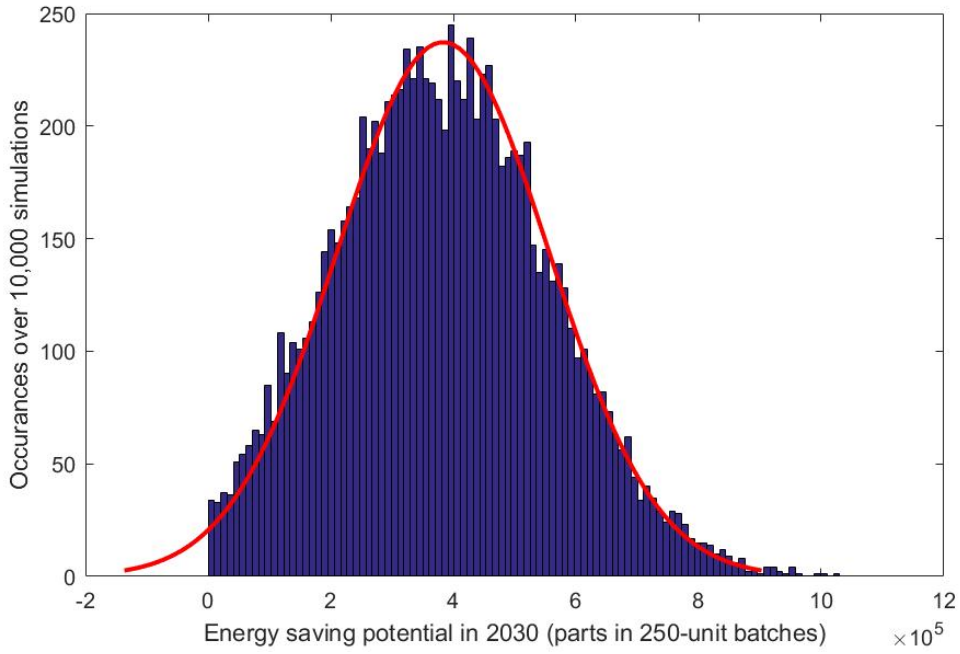

Figure S7: Energy saving potential (parts per year) of ISF for 250-unit batches by 2030. Distribution from 10,000 simulations

The distribution has a kurtosis of 2.9. The closest normal distribution (determined by Matlab) has a mean of 380,000 parts and a standard deviation of 170,000 parts.

As shown in Table 2 of the main manuscript, only 24 to 27 of the parts in a vehicle made during car development (250-unit batches) are both cheaper and less energy intensive to make using ISF than matched die drawing. Hence, the distribution for the number of parts (in 250-unit batches) for which ISF will save energy and money is given in equation S13.

$$X_{250\ \text{unit batch energy \& cost saving potential}}\ [parts/year] \sim 250 \times N(25.5,2.25) \times N(41,400) \quad \text{(S13)}$$

The distribution was calculated by performing 10,000 simulations, each picking a number randomly from the distributions. The result is shown in Figure S8.

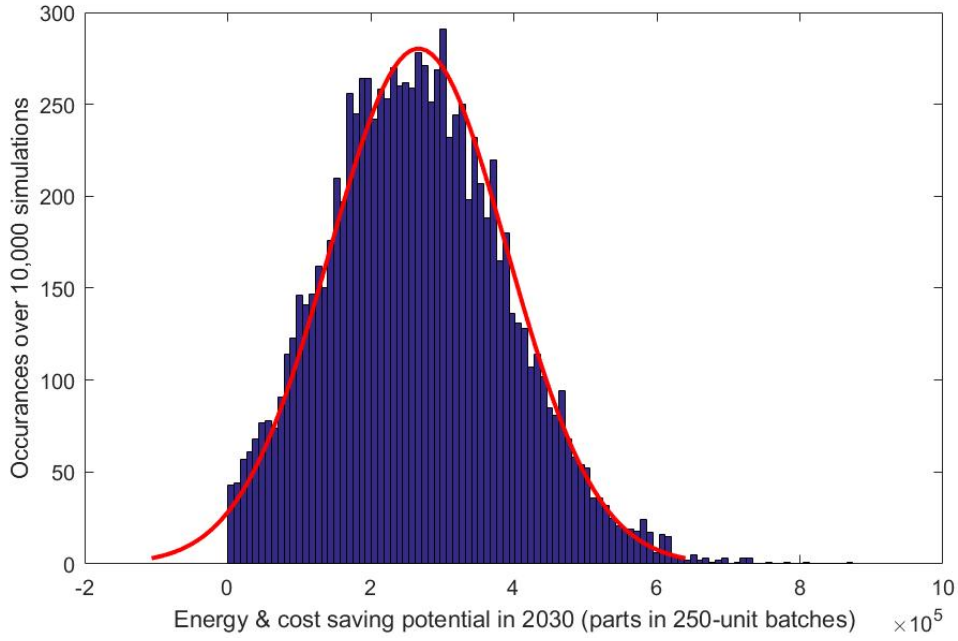

Figure S8: Energy and cost saving potential (parts per year) of ISF for 250-unit batches by 2030. Distribution from 10,000 simulations

The distribution has a kurtosis of 3.1. The closest normal distribution (determined by Matlab) has a mean of 270,000 parts and a standard deviation of 125,000 parts.

4.2 Diffusion of ISF technology: market in 2030

The distributions shown in Figures S6 and S8 correspond to full market penetration of ISF technology across the car industry by 2030. In order to model a more realistic potential, the Bass model was used with the parameters $p \sim N(0.017, 0.0066)$; $q \sim N(0.47, 0.09)$ as described in Section 3.2.3 of the main manuscript. The final distributions were calculated by performing 10,000 simulations each for both the 20-unit and 250-unit batches. The results are shown in Figures S9 and S10.

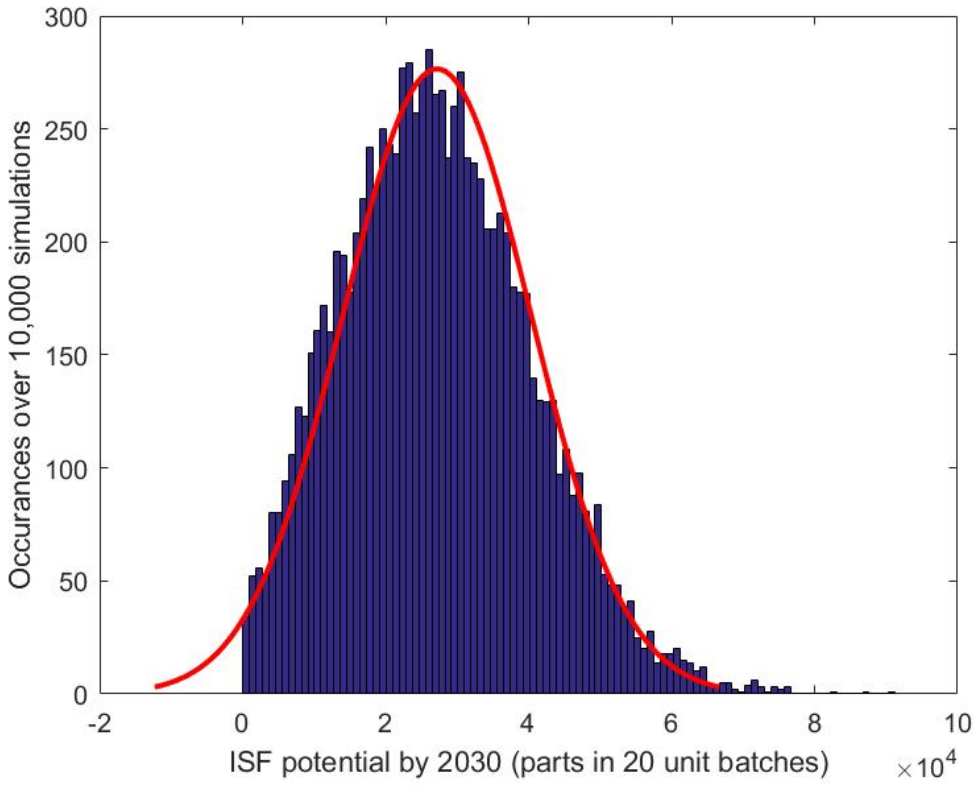

Figure S9: ISF potential by 2030 (parts per year) for parts made during part prototyping (20-unit batches). Distribution from 10,000 simulations

The distribution shown in Figure S9 has a kurtosis of 3.0. The closest normal distribution (determined by Matlab) has a mean of 27,000 parts and a standard deviation of 13,000 parts.

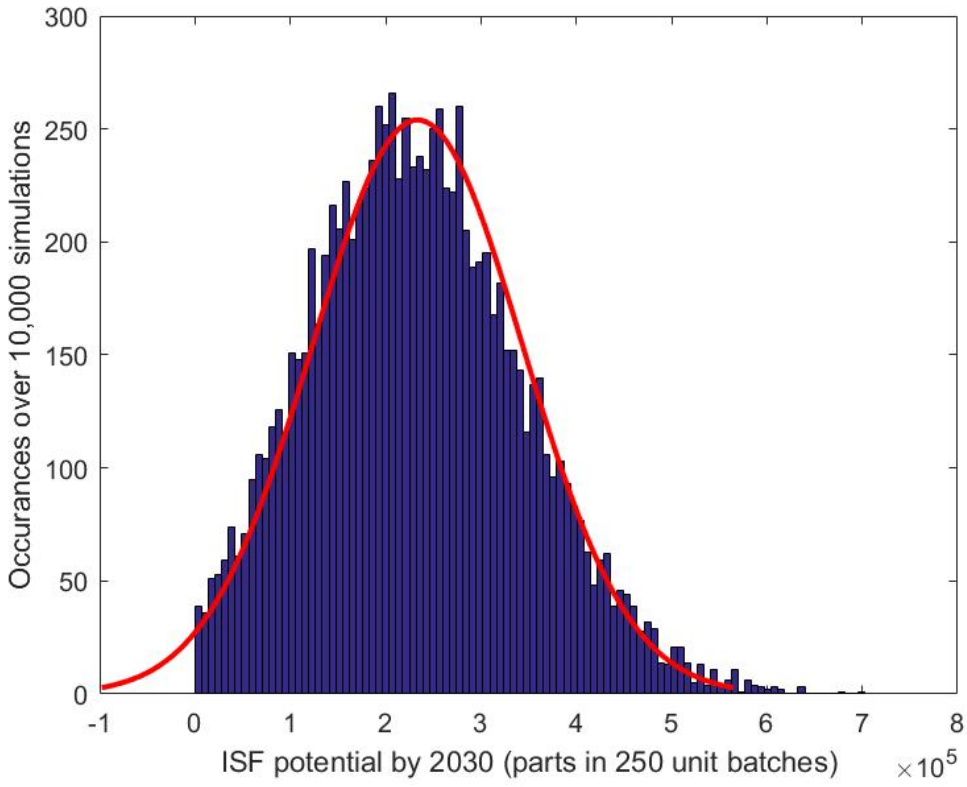

Figure S10: ISF potential by 2030 (parts per year) for parts made during car development (250-unit batches). Distribution from 10,000 simulations

The distribution shown in Figure S10 has a kurtosis of 2.9. The closest normal distribution (determined by Matlab) has a mean of 235,000 parts and a standard deviation of 110,000 parts.

5 Displacement of existing technology and aggregate savings

20-unit batches

Table S4 presents the savings gained by using ISF (instead of zinc drawing dies) to form 20-unit batches of parts across one car development.

Part Description	Interior/exterior	Cost savings (USD/batch)	Energy savings (MJ/batch)	CO2 savings (kgsCO2/batch)
RAFFT candidates (all dimensions equal to or less than 1500mm)				
Front door outer - 2 parts per car	exterior	36634	56573	3203
Rear Door outer - 2 parts per car	exterior	36923	59141	3411
Front Fender - 2 parts per car	exterior	38531	86800	5054
Trunk outer - 1 part per car	exterior	38651	99822	5776
Rear Wheel Well - 2 parts per car	interior	36787	58819	3392
Front door inner - 8 parts per car	interior	35553	28328	1660
Rear door inner - 8 parts per car	interior	35554	26021	1523
A Pillar - 2 parts per car	interior	34772	9763	528
B Pillar - 2 parts per car	interior	34973	17164	969
C Pillar - 2 parts per car	interior	35679	26531	1524
Roof Cross Members - 2 parts per car	interior	34915	14931	808
Trunk - 1 part per car	interior	39364	104163	6087
Total number of parts per vehicle:	**34**	**34**	**34**	**34**
RAFFT candidates (all dimensions fit within 2000 mm x 1500 mm)				
Hood outer - 1 part per car	exterior	42537	176474	10167
Roof outer - 1 part per car	exterior	41871	165024	9570
Firewall (Dash) - 1 part per car	interior	39058	106940	6199
Hood inner - 1 part per car	interior	43559	186850	10948
Rockers - 2 parts per car	interior	35228	25119	1387
Total number of parts per vehicle:	**6**	**6**	**6**	**6**
Savings per vehicle (USD, weeks, MJ, kgsCO2)				
Range of candidate parts (please select):	All			

	Number of part designs (if all parts are candidates)	Cost savings (USD/car)	Energy savings (MJ/car)	CO2 savings (kgsCO2/car)
ISF used wherever technically feasible	**40**	1,462,781	1,983,747	114,765
ISF used to maximize primary energy savings	**40**	1,462,781	1,983,747	114,765
ISF used to maximize cost savings	**40**	1,462,781	1,983,747	114,765
ISF used only when energy and money can be saved	**40**	1,462,781	1,983,747	114,765

Table S4: Savings across one car development (ISF versus zinc die drawing for 20-unit batches – part prototyping)

Across forty 20-unit batches, the total savings are 1,984 $GJ_{primary}$ and 1.46 million USD, equating to 49.6 $GJ_{primary}$ per batch and 36,600 USD per batch. The uncertainty (corresponding to one standard deviation) is equivalent to ±30% of the mean energy saving and ±20% of the mean cost saving. The uncertainty surrounding these savings was estimated by calculating the range of possible savings if a 1.5 m^2, 1.5 mm thick aluminum part was produced in 20-unit batches.

Subsequently, the average energy saving per batch (20-units) ~ $N(49.6,(0.3*49.6)^2)$ GJ

…and the average cost saving per batch (20-units) ~ $N(36000,(0.2*36000)^2)$ USD

The actual savings in 2030 are therefore these per-batch savings multiplied by the distribution of likely batches in 2030 (derived from Figure S9). The final result is presented in Figure S11.

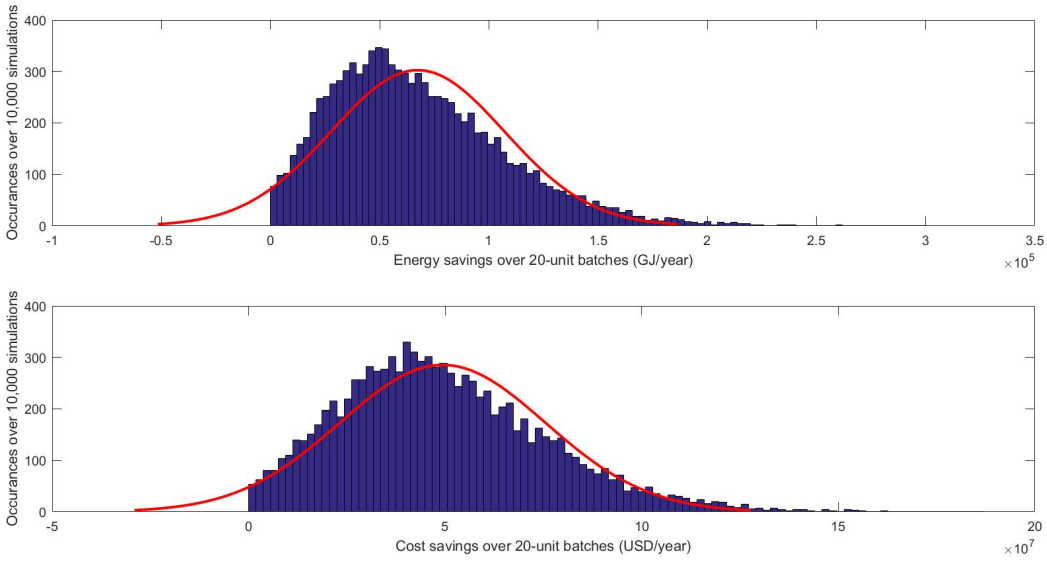

Figure S11: Potential savings by 2030 from using ISF in the car industry to form part prototypes (20-unit batches). Distribution from 10,000 simulations

The energy and cost distributions shown in Figure S11 have kurtosis values of 4.0 and 3.6, respectively. The mean energy savings are 67 TJ (standard deviation of 40 TJ). The mean cost savings are 49 million USD (standard deviation of 26 million USD).

250-unit batches

Table S5 presents the savings gained by using ISF (instead of zinc drawing dies) to form 250-unit batches of parts across one car development.

Analysis of Sheet metal parts on passenger car				
Part Description	**Interior/exterior**	**Cost savings (USD/batch)**	**Energy savings (MJ/batch)**	**CO2 savings (kgsCO2/batch)**
RAFFT candidates (all dimensions equal to or less than 1500mm)				
Front door outer - 2 parts per car	exterior	7691	-32295	-2773
Rear Door outer - 2 parts per car	exterior	11865	9277	367
Front Fender - 2 parts per car	exterior	14712	61133	3896
Trunk outer - 1 part per car	exterior	5094	34302	1944
Rear Wheel Well - 2 parts per car	interior	10170	5256	138
Front door inner - 8 parts per car	interior	17556	12806	996
Rear door inner - 8 parts per car	interior	19233	12416	919
A Pillar - 2 parts per car	interior	18912	-29646	-2186
B Pillar - 2 parts per car	interior	16423	-22453	-1611
C Pillar - 2 parts per car	interior	19685	-167	-155
Roof Cross Members - 2 parts per car	interior	16249	-40883	-3073
Trunk - 1 part per car	interior	14008	88565	5828
Total number of parts per vehicle:	**34**	**34**	**24**	**24**
RAFFT candidates (all dimensions fit within 2000 mm x 1500 mm)				
Hood outer - 1 part per car	exterior	-865	63382	3044
Roof outer - 1 part per car	exterior	833	90910	5463
Firewall (Dash) - 1 part per car	interior	5721	47429	2840
Hood inner - 1 part per car	interior	11920	193081	12804
Rockers - 2 parts per car	interior	12376	-46260	-3517
Total number of parts per vehicle:	**6**	**5**	**4**	**4**
Savings per vehicle (USD, weeks, MJ, kgsCO2)				
Range of candidate parts (please select):	All			

	Number of part designs (if all parts are candidates)	**Cost savings (USD/car)**	**Energy savings (MJ/car)**	**CO2 savings (kgsCO2/car)**
ISF used wherever technically feasible	**40**	587,195	527,365	29,419
ISF used to maximize primary energy savings	**28**	404,523	870,773	56,047
ISF used to maximize cost savings	**39**	588,059	463,983	26,375
ISF used only when energy and money can be saved	**27**	405,388	807,391	53,004

Table S5: Savings across one car development (ISF versus zinc die drawing for 250-unit batches – car development)

Across twenty-seven 250-unit batches, the total savings are 810,000 $MJ_{primary}$ and 405,000 USD, equating to 30 $MJ_{primary}$ per batch and 15,000 USD per batch.

Subsequently, the average energy saving per batch (20-units) ~ $N(810,(0.3*810)^2)$ GJ

…and the average cost saving per batch (20-units) ~ $N(15000,(0.2*15000)^2)$ USD

The actual savings in 2030 are therefore these per-batch savings multiplied by the distribution of likely batches in 2030 (derived from Figure S10). The final result is presented in Figure S12.

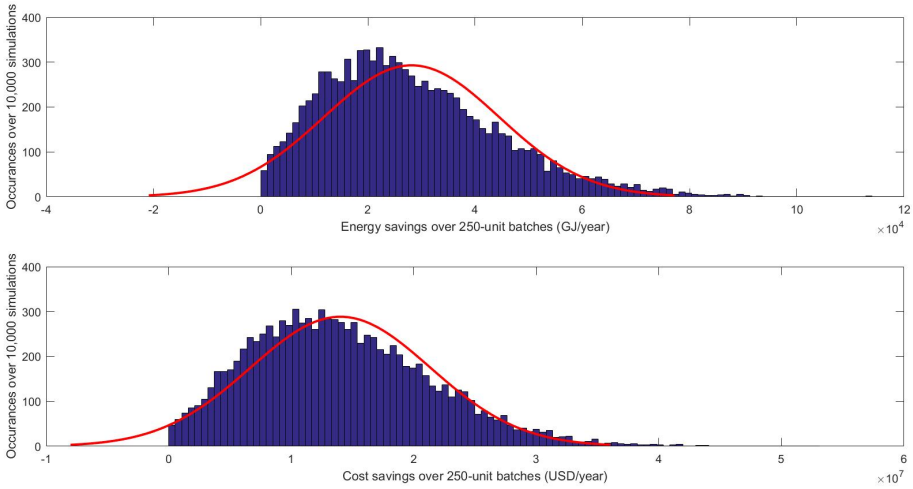

Figure S12: Potential savings by 2030 from using ISF in the car industry to form car development parts (250-unit batches). Distribution from 10,000 simulations

The energy and cost distributions shown in Figure S12 have kurtosis values of 3.6 and 3.0 respectively. The mean energy savings are 28 TJ (standard deviation of 16 TJ). The mean cost savings are 14 million USD (standard deviation of 7 million USD).

6 Practical applications of ISF: interviews conducted

In order to evaluate if one-to-one displacement is a realistic scenario, a series of interviews were conducted with industry experts: zinc die manufacturers, prototype part makers, design engineers, and managers at prototyping facilities. A list of the interviewees and questions that guided the discussions are provided in Table S6.

Questions that guided the conversation:

- Given ISF reaches the desired specifications [shown in Table 1 of main manuscript], how do you envision it could change your business/what you do?
- Could you envisage ISF replacing zinc die-sets?
- Does technology exist (other than ISF) which may also displace the zinc die drawing process?

- What are the advantages of using zinc drawing dies?
- If the new ISF technology is cost and energy competitive, are there any reasons you would continue using the existing technology?

Interviewee	Company
Supervisor at "Global Prototyping"	Ford Motor Company
Manager at "New Model Product Development Center"	Ford Motor Company
Round table meeting with industrial and design engineers at a prototype die making company	Troy Design and Manufacturing
President of company specializing in forming of automotive body panels for low-volume and niche vehicles using hydroforming technology and ISF variants	Amino North America
President of company that provides prototype automotive stamping parts	Oakley Industries

Table S6: How will RAFFT, if successfully developed, be used in the car industry? List of semi-structured interview questions and interviewees

A consensus emerged from the interviews that ISF could supersede matched die drawing for part prototyping (20-unit batches) because the potential cost savings are large. However, it was deemed unlikely that in the foreseeable future ISF will completely supersede zinc die drawing for car development (250-unit batches). This is partly because car companies use the experience of drawing the 250-unit batches to inform the final design of both the part and the steel/iron drawing dies that will be used in mass production. ISF would be a poor indicator of material behavior during mass production because the forming mechanics in ISF differ significantly from those in drawing. Improved finite element simulations may reduce the need for this learning step in the future.

References

Brodrick, J. R. (2010). Energy Savings Potential of Solid-State Lighting in General Illumination Applications 2010 to 2030. *Energy*, (February), 1–54.

Cooper, D., & Gutowski, T. (2016). *Rapid Freeform Sheet Metal Forming: Potential environmental and economic benefits*. Cambridge, Ma.

Cooper, D. R., Rossie, K. E., & Gutowski, T. G. (2017). The energy requirements and environmental impacts of sheet metal forming: an analysis of five forming processes. *Journal of Materials Processing Technology*.

Das, S., Graziano, D., Upadhyayula, V. K. K., Masanet, E., Riddle, M., & Cresko, J. (2016). Vehicle lightweighting energy use impacts in U. S. light-duty vehicle fleet. *SUSMAT*. http://doi.org/10.1016/j.susmat.2016.04.001

DeForest, N., Shehabi, A., O'Donnell, J., Garcia, G., Greenblatt, J., Lee, E. S., … Milliron, D. J. (2015). United States energy and CO2 savings potential from deployment of

near-infrared electrochromic window glazings. *Building and Environment*, *89*, 107–117. http://doi.org/10.1016/j.buildenv.2015.02.021

Greenblatt, J. B., & Saxena, S. (2015). Autonomous taxis could greatly reduce greenhouse-gas emissions of US light-duty vehicles. *Nature Climate Change*, *5*(July). http://doi.org/10.1038/nclimate2685

Huang, R., Riddle, M., Graziano, D., Warren, J., Das, S., Nimbalkar, S., … Masanet, E. (2015). Energy and emissions saving potential of additive manufacturing: the case of lightweight aircraft components. *Journal of Cleaner Production*. http://doi.org/10.1016/j.jclepro.2015.04.109

Levy, J. I., Woo, M. K., & Tambouret, Y. (2016). Energy savings and emissions reductions associated with increased insulation for new homes in the United States. *Building and Environment*, *96*, 72–79. http://doi.org/http://dx.doi.org/10.1016/j.buildenv.2015.11.008

PRé Consultants. (2013). *Pré, 2013. Simapro Database Manual: Methods Library. Version 2.5. , October*.

Rossie, K. (2015). *An energy and environmental analysis of aerospace sheet metal part manufacturing*. Master of Science thesis. Massachusetts Institute of Technology.

Shehabi, A., Deforest, N., McNeil, A., Masanet, E., Greenblatt, J., Lee, E. S., … Milliron, D. J. (2013). U.S. energy savings potential from dynamic daylighting control glazings. *Energy and Buildings*, *66*, 415–423. http://doi.org/10.1016/j.enbuild.2013.07.013